

Competitive Adsorptive Removal of Pb, Cu and Cd from Water Using Water Pennywort Fixed on Alginate

Mahamadi C^{1*}, Mupa M² and Jackson GE³

¹Research and Postgraduate Centre, Bindura University of Science Education, P. Bag 1020, Bindura, Zimbabwe

²Chemistry Department, Bindura University of Science Education, P. Bag 1020, Bindura, Zimbabwe

³Department of Chemistry, University of Cape Town, Rondebosch 7700, South Africa

Abstract

The adsorption of Pb (II), Cu (II) and Cd (II) on immobilized water pennywort-*Hydrocotyle ranunculoides* was investigated in batch and continuous flow systems. Physical characterization of adsorbent was performed using fourier transform infrared (FT-IR) spectroscopy and scanning electron microscopy (SEM). Analysis of batch sorption data using single component and competitive Langmuir models showed that maximum equilibrium sorption capacities for single-metal systems followed the trend (mg/g): Pb(II) (22.25)>Cu(II) (12.55)>Cd(II) (11.45). Mutual interference was probed using normalised equilibrium adsorption capacities, q_e'/q_e , where the prime indicates the presence of the other metal ion. The results showed that removal of Cu (II) and Cd(II) ions was severely suppressed in the presence of Pb(II) whereas the removal of Pb(II) in the presence of Cu(II) and Cd(II) ions was still effective. Adams-Bohart and Thomas models were used to study the effect of important parameters: bed depth (1.5-2.5 cm), flow rate (2-20 ml/min) and initial metal concentration (10-100 mg/l). It was shown that the Thomas model provided a better fit to the experimental data indicating that mass transfer, i.e. external diffusion was not the rate limiting steps. In conclusion, immobilised *H. ranunculoides* proved to be a potential biosorbent for the removal of heavy metal ions from aquatic environments.

Keywords: *Hydrocotyle ranunculoides*; Continuous flow; Binary sorption; Lead; Copper; Cadmium

Introduction

The question of toxicity and health hazards associated with heavy metal accumulation in aquatic systems has generated sustained research over centuries. Biosorption, the process of passive cation binding by dead or living biomass, represents a potentially cost-effective way of eliminating toxic heavy metals from industrial waste waters. The initial incentives of biosorption development for industrial processes include the low cost of biosorbents, their great efficiency for metal removal at low concentration, potential for biosorbent regeneration and metal recovery, high velocity of sorption and desorption, limited generation of secondary residues, and more environmentally friendly life cycle of the material [1].

The complexity of the biochemistry of the biosorbents has led to numerous interpretations on the mechanisms involved in the biosorptive accumulation of metal ions [2]. However, it has generally been agreed that metal binding takes place through electrostatic interaction, surface complexation, ion-exchange, and precipitation which can occur individually or combined [3]. On parameters that affect biosorption, it has generally been observed that temperature does not influence biosorption between 20 and 35°C whereas pH affect biosorption through its influence on metal chemical speciation, the activity of biomass functional groups, and the ion metallic competition sites [4]. In dilute solutions, biomass concentration has been found to have an influence on biosorption capacity with an increase in biosorption being observed at lower concentrations.

Although much research has been carried out on the uptake of heavy metal ions by many researchers, this has been largely limited to single-metal adsorption. However, under most conditions, wastewater streams contain more than one kind of metal ions and examining the interactive effects of divalent cations in various combinations is more representative of the actual environmental problems faced by organisms

than the studies of a single metal. As a result, multicomponent or competitive adsorption of metals from water solution has been investigated on various adsorbents in the last decade. The following multicomponent adsorption systems have been studied: Cu(II)-Cd(II) on chitosan cross-linked with epichlorohydrin-triphosphate [5]; Cu(II)-Zn(II) on *Myriophyllum spicatum* [6] Cu(II)/Pb(II)-Cd(II) on immobilized *Lentinus edodes* residues [7]; Zn(II)-Cd(II)-Ni(II)-Cu(II)-Cr(III) on clay-bearing mining wastes [8]; Pb(II)-Zn(II) on sulfured orange peel [9]; and Cu(II)-Pb(II) on activated carbon obtained by pyrolysis of cow bone [10]. In a study of the competitive adsorption of Pb²⁺ and Zn²⁺ onto activated carbon derived from van apple pulp, it was found that individual metal ions adsorption decreased whilst more metal ions were adsorbed in multi-metal solutions [11]. Binary and ternary sorption of Pb²⁺, Cd²⁺ and Zn²⁺ ions onto *Eichhornia crassipes* showed that the combined action of the metals was antagonistic and the metal sorption followed the order Pb²⁺>>Cd²⁺>Zn²⁺ [12]. The same authors also observed that Pb²⁺ ions could still be effectively removed in the presence of Zn²⁺ and Cd²⁺ ions, but the removal of Cd²⁺ and Zn²⁺ ions would be suppressed in the presence of Pb²⁺ ions. Zhu et al. [13], carried out sorption studies of Pb²⁺, Cu²⁺, and Zn²⁺ from ternary solutions onto xanthate-modified magnetic chitosan and reported that the adsorption capacities followed the order: Pb²⁺>Cu²⁺>Zn²⁺. More recently, Sulaymon et al. [14] observed that the biosorption capacity for single metals onto activated sludge decreased by 11-51%, 53-88% and

*Corresponding author: Mahamadi C, Research and Postgraduate Centre, Bindura University of Science Education, P. Bag 1020, Bindura, Zimbabwe, Tel: +26377350801; E-mail: cmahamadi@buse.ac.zw

Received June 07, 2015; Accepted June 24, 2015; Published June 26, 2015

Citation: Mahamadi C, Mupa M, Jackson GE (2015) Competitive Adsorptive Removal of Pb, Cu and Cd from Water Using Water Pennywort Fixed on Alginate. J Bioremed Biodeg 6: 300. doi:10.4172/2155-6199.1000300

Copyright: © 2015 Mahamadi C, et al. This is an open access article distributed under the terms of the Creative Commons Attribution License, which permits unrestricted use, distribution, and reproduction in any medium, provided the original author and source are credited.

79-94% in the binary, ternary and quaternary systems respectively at the optimum agitation speed of 600-800 rpm.

In many cases, biosorption studies have been carried out using native biomasses and products obtained from biomasses, which are generally biopolymers (polysaccharides and glycoproteins). Use of biosorbents in native forms from microbial biomasses (e.g. yeasts, microalgae, bacteria, etc.) has some drawbacks such as difficulties on separation of cells after the biosorption, mass loss during the separation, and the low mechanic resistance of the cells [15]. Several techniques exist which can make biosorbents suitable for process applications. Among these, adsorption on inert supports by preparation of biofilms; encapsulation in polymeric matrices as calcium alginate, polyacrylamide, polysulfone, and polyhydroxyethylmetacrylate; covalent linkage on supports by chemical agents; and crosslinking by chemical agents that form stable cellular aggregated have been found to be practical for biosorption [16].

The present work studies for the first time, the immobilization of *H. ranunculoides* root and stem biomass in calcium alginate and its potential use as a biosorbent in batch and continuous-flow systems. The perennial plant occurs abundantly at Lake Chivero in Zimbabwe where its extensive mats disrupt ecology and poses a threat to recreational uses of the waterways. The high abundance of the plant makes its possible conversion into chemically and physically stable beads to be an attractive option for removal of toxic metals from aquatic environments. The alginate-*H. ranunculoides* beads are investigated for their ability to remove Pb(II), Cd(II) and Cu(II) from binary solutions in batch system and from single metal solutions in continuous system.

Materials and Methods

Reagents

Sodium alginate, calcium chloride, copper sulphate, lead nitrate and cadmium chloride were purchased from Sigma Aldrich, Germany. Heavy metal stock solutions (1000 ppm) were separately prepared by dissolving analytical grade $\text{CuSO}_4 \cdot 5\text{H}_2\text{O}$, $\text{Pb}(\text{NO}_3)_2$, $\text{CdCl}_2 \cdot 2.5\text{H}_2\text{O}$ in deionised water. Solutions of different concentrations were obtained by diluting the stock solution.

Biosorbent preparation

H. ranunculoides samples were collected from Lake Chivero, near Harare, Zimbabwe. Root and stem samples were washed with running tap water to remove sand and grit, rinsed with deionised water and sun dried. The samples were then ground to a fine powder using mortar and pestle and sieved through mesh of size less than or equal to 150 μm . Acid pretreatment of the biomass was then followed by agitating approximately 5 g of the biomass for every 100 ml of 1 M HCl for 12 hr. After HCl treatment the biomass was collected by filtration under vacuum suction. This was followed by washing with de-ionised water to remove excess acid. The process was repeated 5 times before drying the biomass at 40°C in an oven until constant weight.

The dried biomass powder was fixed on alginate using a method described by Vijayaraghavan and Yuan [17]. A 2% (w/v) polymer solution was prepared by dissolving 2 g of Sodium alginate for every 100 g of deionised water and then shaking for 24 hr at 300 rpm to make a homogenous polymer solvent mixture. Two grams of the biomass powder was then blended with 100 ml of the 2% (w/v) sodium alginate solution which was then extruded dropwise through a funnel into 0.1 M calcium chloride solution to make beads with a biomass loading of 2% and dimensions of 3 to 5 mm in diameter. The beads were hardened by placing them in 2% calcium chloride solution for 12 hr. Those

that floated on the surface were discarded. The remaining beads were washed by agitation in deionised water at 100 rpm in 250 ml conical flasks for 30 min, discarding the solution, and then repeating the process 5 times until the conductivity the resulting filtrate approached that of the deionised water. After removing residual water with paper towels the beads were dried gradually at room temperature to constant weight and then used for further experiments.

Biosorbent characterization

Scanning electron microscopy (SEM) morphologies were done in an FEI Nova Nano SEM 230 instrument (Holand) and images were acquired at magnification of 500x, 2000x, and 10000x. IR studies were carried out using a Perkin-Elmer Spectrum 100 FT-IR over a range of 4000-4500 cm^{-1} . Specific surface area was determined according to the Brunaru Emmet-Teller (BET) protocol on a Micromeritics model ASAP 2000. The point of zero charge (pH_{pzc}) of the adsorbent was determined using the method described by Ofomaja and Ho [18].

Adsorption column

The column used was a glass tube with an inner diameter=1.2 cm, outer diameter=1.83 cm, length=30 cm. An adjustable plunger was attached with a 20 μm filter of 1.1 mm thickness at the top of the column, and a stainless sieve with a mesh size of 70 (0.5 mm) was placed at the bottom. The following parameters were kept constant throughout the studies: bulk density (0.25 g/cm^3), packing density (1.2 g/cm^3), void fraction (0.25), exchangeable calcium (130 mg/g) and biomass loading of 5%.

Batch biosorption experiments

Biosorption experiments onto alginate-*H. ranunculoides* beads were conducted in 250 ml flasks containing 50 ml of single-component or binary mixtures of heavy metal solutions and 0.1 g of biomass. Initial pH was adjusted to 5.5 using 0.1 M HNO_3 or 0.1 M NaOH. Binary metal mixtures [Pb(II)-Cd(II), Pb(II)-Cu(II) and Cd(II)-Cu(II)] were made for combinations of the metals in the ratios; 1:1, 1:2 and 2:1 respectively by mixing appropriate quantities of the metal solutions as reported by Mahamadi and Nharingo [12]. For example, a 1:1 Cu(II)- Pb(II) mixture was prepared by making a composite mixture comprising of 10 mg/l Cu(II) and 10 mg/l Pb(II) respectively and a 1:2 Cu(II)-Pb(II) mixture was prepared by making a composite mixture comprising of 10 mg/l Cu(II) and 20 mg/l Pb(II) respectively. The mixtures were shaken on a rotary shaker (agitation rate, 150 rpm) for a predetermined equilibrium period of 6 h. The biosorbent was then filtered through an acid-cleaned 0.45 μm Millipore filter and the concentrations of heavy metal ions in the filtrate were analysed by flame atomic absorption spectrometry. The amount of heavy metal ions uptake by the beads in each flask was determined using the mass balance equation:

$$q = \left(\frac{C_0 - C_e}{W} \right) \quad (1)$$

where q is the adsorption amount at equilibrium (mg/g); C_0 is the initial metal concentration (mg/L); C_e is the concentration remaining in solution at equilibrium (mg/l); W is biosorbent dose (g/l). Metal ion concentration in the exiting solution was determined using a Varian AA- 1275 Spectrometer.

Column biosorption tests

In all column experiments, packing density was kept at approximately value of 1.0 g/cm^3 by measuring the appropriate mass of the beads for a given bed depth. Metal solutions were prepared as described for batch experiments. A flowrate of 5 ml/min was

delivered by an EYELA Microtube MP-3 (Japan) peristaltic pump and controlled by a flow-meter (Dwyers) and in-line flow-pulse dampener. Metal ion concentration was determined by flame atomic absorption spectrometry.

Results and Discussion

Characterization of the adsorbent

The FT-IR spectrum of alginate-*H. ranunculoides* is given in Figure 1. The strong and very broad peak at 3632.47-2963.14 cm^{-1} indicates the stretching vibrations of a hydrogenbonded O-H group. The peak at 1600.43 is due to the bending vibrations of an amine N-H group or aromatic C=C. The presence of an aromatic ring is further suggested by the peak occurring at 1420.07. Weak bands at 1319.88, 1263.76, and 1155.55 cm^{-1} are due to a C-O stretch and suggest the presence of an acyl C-O, phenol C-O, or alkoxy C-O. The presence of an alkoxy C-O is further confirmed by the strong peak at 1031.3 cm^{-1} . The band centred at ca. 560 cm^{-1} was associated with out-of-plane bending vibrations of C-H or O-H group [19]. The SEM images of alginate-*H. ranunculoides* are shown in Figure 2 and they clearly reveal the polysaccharide nature

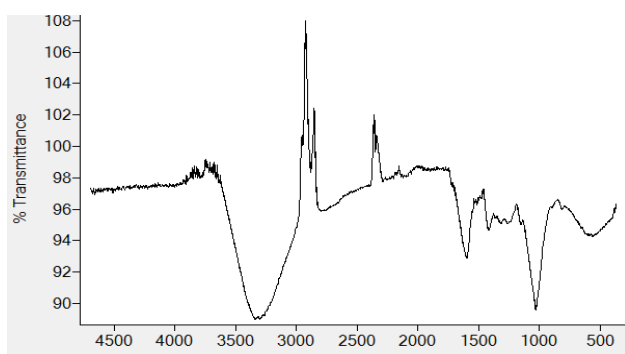


Figure 1: FT-IR spectrum of alginate-*H. ranunculoides*.

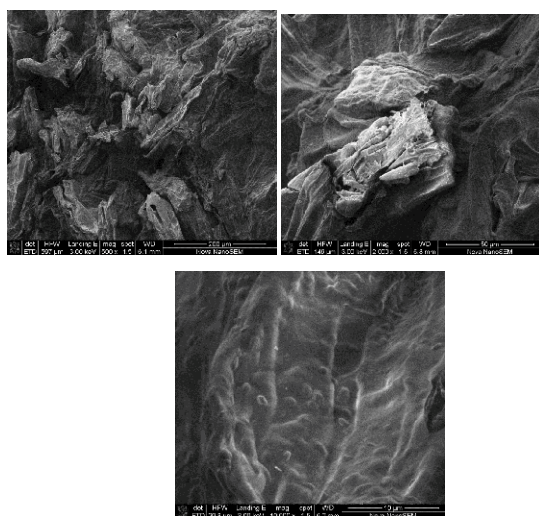


Figure 2: SEM images of alginate-*H. ranunculoides*.

of the adsorbent having a network of organized fibers. A pH_{pzc} value of 4.7 was obtained which shows that cations adsorption would be favourable at pH values higher than 4.7, and anions adsorption at pH values lower than pH_{pzc} . Consequently, all adsorption experiments for metal sorption were carried out at an initial pH of 5.5. A BET surface area of 11.2 m^2/g was obtained for alginate-*H. ranunculoides*, which is comparable to that reported for polyaniline grafted chitosan beads [20].

Monocomponent adsorption

The equilibrium of the adsorptive removal of the metals from single-component systems was described by fitting data to Langmuir model expressed in a linearized form as follows:

$$C_e/q_e = \frac{1}{q_{\text{max}}b} + \frac{C_e}{q_{\text{max}}} \quad (2)$$

where q_e (mg/g) is the equilibrium sorption capacity; q_{max} (mg/g) is the maximum amount of metal ion per unit weight of the alginate-*H. ranunculoides* beads required to form a complete monolayer on the surface, and b is the equilibrium adsorption constant which is related to the affinity of the binding sites.

Figure 3 shows plots of q_e vs C_e for the sorption of Pb(II), Cu(II) and Cd(II) ions by alginate-*H. ranunculoides* beads. The results indicated that the adsorptive capacity of alginate-*H. ranunculoides* beads to hold Pb(II) ions was larger than for Cu(II) and Cd(II) ions. Similar results were observed for the removal of Pb(II) and Cu(II) by *Mansonia* sawdust [21]. Furthermore, Equation 2 was fitted to the experimental data and the results are shown in Figure 4. From linear regression, it was shown in Table 1 that the maximum adsorption capacities, q_{max} , for mono-component sorption followed the trend: Pb(II) (22.25 mg/g) > Cu(II) (12.55mg/g) > Cd(II) (11.45 mg/g). Higher q_{max} value for Pb confirms the stronger bonding affinity of alginate-*H. ranunculoides* beads towards Pb(II) than Cu(II) or Cd(II). Similar findings were reported for metal sorption by BMSZ711 [22,23].

Batch binary sorption

The nature of competitive adsorption in two-metal systems was analysed using the Langmuir competitive model [24]:

$$q_{e,i} = q_{\text{max},i} K_{L,i} C_{e,i} \left(1 + \sum_{j=1}^n K_{L,j} C_{e,j} \right)^{-1} \quad (3)$$

where $q_{\text{max},i}$ and $K_{L,i}$ are physical parameters, and $C_{e,i}$ are equilibrium concentrations in the mixture of the solutes. It can be shown that in a system where the concentrations of the solutes are

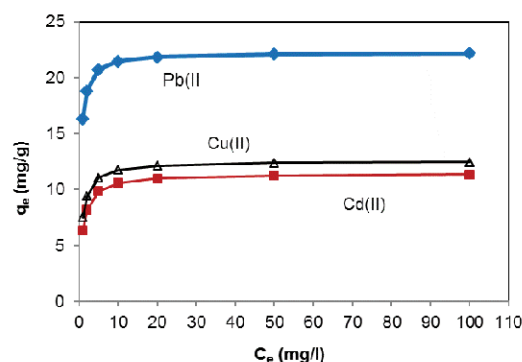
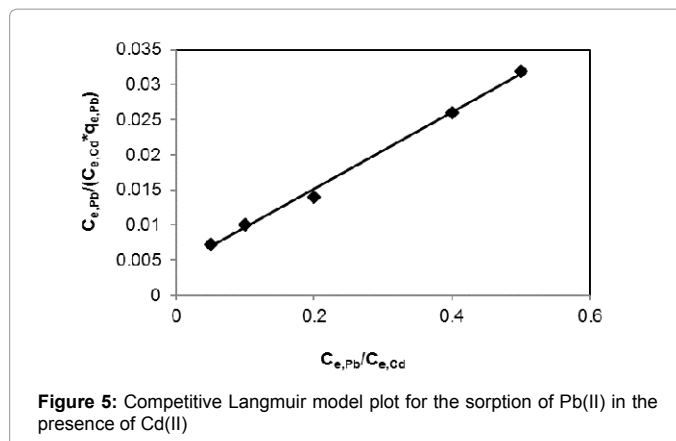
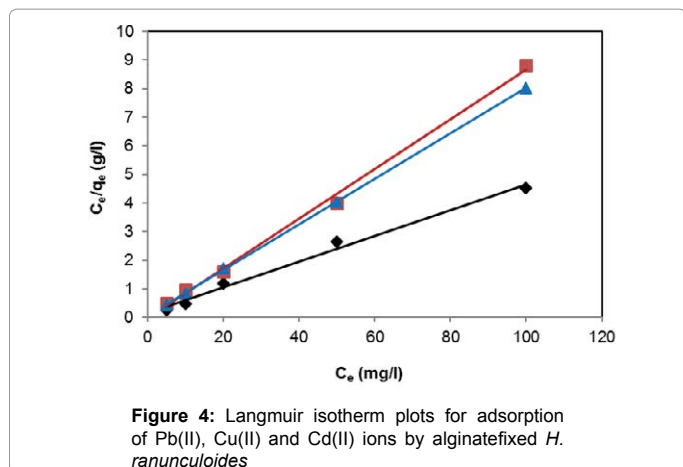


Figure 3: Plots of q_e vs C_e for the adsorption of Pb(II), Cu(II) and Cd(II) by alginate-fixed *H.ranunculoides*.



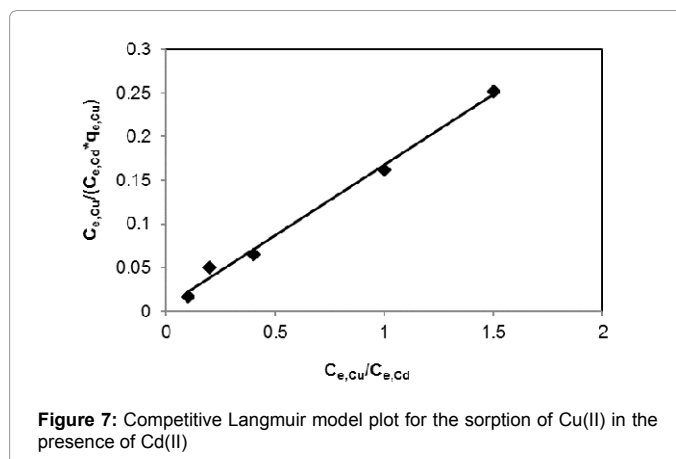
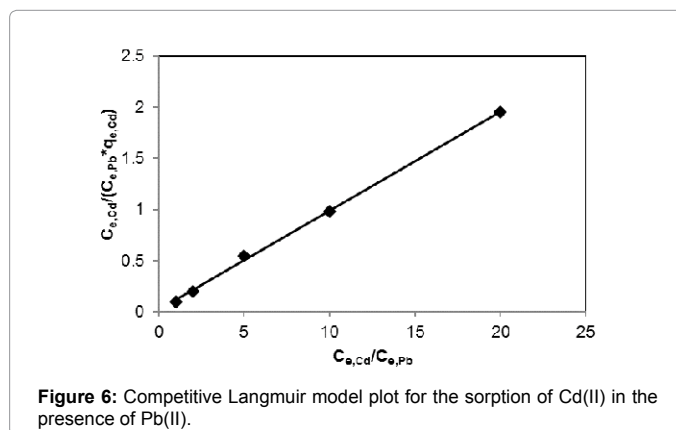
Metal ion (+interferent)	q _e , exp. (mg/g)	b (l/mg)	q _{max} (mg/g)	q _e /q _e
(a) Pb as primary metal ion				
Pb	13.21; R ² =0.988	0.3	22.22	1
Pb-Cd (1:1)	9.56; R ² =0.996		18.23	0.72
Pb-Cd (2:1)	16.28		24.42	1.23
Pb-Cd (1:2)	4.76		10.23	0.36
Pb-Cu (1:1)	7.15		21.46	0.54
Pb-Cu (2:1)	19.56		23.56	2.74
Pb-Cu (1:2)	5.4		9.86	0.76
(b) Cd as primary metal				
Cd	6.48; R ² =0.996	7.38	11.48	1
Cd-Pb (1:1)	3.32; R ² =0.998		10.23	0.51
Cd-Pb (2:1)	11.33		13.59	1.75
Cd-Pb (1:2)	4.61		7.86	0.71
Cd-Cu (1:1)	6.06		5.05	0.94
Cd-Cu (2:1)	11.69		7.23	1.92
Cd-Cu (1:2)	4.53		4.36	0.7
(c) Cu as primary metal				
Cu	6.55; R ² =0.999	1.21	12.56	1
Cu-Pb (1:1)	4.98		4.56	0.76
Cu-Pb (2:1)	12.31		7.53	1.88
Cu-Pb (1:2)	5.02		5.04	0.76
Cu-Cd (1:1)	5.01; R ² =0.993		6.18	0.94
Cu-Cd (2:1)	13.3		10.42	2.03
Cu-Cd (1:2)	6.19		4.48	0.95

Table 1: Single and binary system adsorption parameters obtained using the langmuir monocomponent and langmuir competitive models.

sufficiently large that surface coverage is substantially complete, the unit term in Equation 1 may be neglected and the equation can be linearized as follows:

$$\frac{C_{e,1}}{C_{e,2}q_{e,1}} = \frac{C_{e,1}}{q_{max,1}C_{e,2}} + \frac{K_{L,2}}{K_{L,1}q_{e,1}} \quad (4)$$

Results of the plots of $C_{e,1}/C_{e,2}q_{e,1}$ as a function of $C_{e,1}/C_{e,2}$ for the sorption of Pb(II) in the presence of Cd(II), Cd(II) in the presence of Pb(II), and Cu(II) in the presence of Cd(II) are shown in Figures 5-7 and the model parameters are given in Table 1. The equilibrium sorption capacity of one metal in the presence of another, q_e , was normalized to that in the absence of the other metal, q_e , and q_e/q_e the ratios were used to probe the sorption dynamics.



The normalized sorption ratios, q_e/q_e for the sorption of one metal in the presence of another metal are shown in Table 1. For binary systems of equal metal concentrations (1:1), the ratios were all <1, indicating that the adsorption of the metals was depressed by the presence of other metals in the binary solution. These results suggest that the effects of the mixtures were antagonistic. Furthermore, the q_e/q_e ratios for the sorption of Pb(II) ions in the presence of Cu(II) and Cd(II) ions were 0.54 and 0.72, respectively suggesting that Cu(II) ions had a higher depressive effect on the sorption of Pb(II) ions by alginate-*H. ranunculoides*. Similar observations were made for the Pb(II)-M (2:1 and 1:2) compositions (where M=Cd(II) or Cu(II)). It is noteworthy that when the concentration of Pb(II) was doubled relative to Cd(II) or

Cu(II), it became increasingly difficult for the adsorbent to sequester Cd(II) or Cu(II) ions respectively. These findings indicate that the observed selectivity was not only related to metal ionic characteristics of the species present but was also related to the concentration ratio of the ions present in solution considering the all other environmental factors were held constant. It was also observed that sorption of Cu(II) ions was more significantly depressed in the presence of Pb(II) ions than in the presence of Cd(II) ions and similar findings were made for the sorption of Cu(II) ions. It may also be interesting to note that the overall adsorption capacities of alginate-*H. ranunculoides* for Pb(II)-Cd(II) (9.56 + 3.32) and Pb(II)-Cu(II) (7.15 + 4.98) mg/g were higher than that of Cd(II) (6.48 mg/g) and Cu(II) (6.55 mg/g) but lower than that of Pb(II) (13.21 mg/g) in single-metal sorption. A possible explanation is that there could be partial overlap between the adsorption sites of Pb(II) and those of Cd(II) and Cu(II) ions in binary systems.

Single and binary system adsorption parameters obtained using the Langmuir Monocomponent and Langmuir Competitive Models (Table 1).

Continuous flow sorption

Breakthrough curves: The breakthrough curves for the sorption of Pb(II), Cu(II) and Cd(II) ions by alginate-*H. ranunculoides* are shown in Figure 8. The breakthrough times are estimated to be 20, 22, and 35 h, whilst saturation times were 75, 90 and 120 h for the adsorption of Cd(II), Cu(II) and Pb(II) ions respectively. Furthermore, it is noteworthy that the curves were steeper for the adsorption of Cu(II) and Cd(II) ions than for Pb(II) ion, which was characterized by a broadened mass transfer zone. The closeness in the breakthrough times for Cu(II) and Cd(II) is consistent with the closeness in the batch monolayer maximum adsorption capacities as shown in Table 1 and Figure 8.

Dynamic adsorption models: The concentration profiles in the liquid and solid phases change in space and time during column adsorption. Therefore, from perspective of design and optimization of the column processes, it is important to predict the breakthrough curve for the effluent. Numerous fixed bed models have been formulated at different levels of complexity in the modeling of environmental sorption and biosorption research [25]. These include the mass transfer, Adams-Bohart, Thomas, Yoon Nelson, Bed Depth Service Time model, etc. In this study, Adams-Bohart and Thomas models were applied to analyze the experimental data.

Adams-Bohart model: The Adams-Bohart model is used only for

the description of the initial part of the breakthrough curve, i.e. up to 10-50% of the saturation point [26]. In this model, it is assumed that the adsorption process is continuous and that equilibrium is not attained instantaneously and the most commonly used form of the model is shown in Eq. 5.

$$\ln \frac{C_t}{C_o} = k_{AB} C_o t - k_{AB} N_o \frac{Z}{U_o} \quad (5)$$

where C_o and C_t are the inlet and outlet adsorbate concentrations (mg l^{-1}) respectively, Z is the bed height (cm), U_o is superficial velocity (cm min^{-1}), defined as the ratio of the volumetric flowrate Q ($\text{cm}^3 \text{min}^{-1}$) to the cross-sectional area of the bed A (cm^2), K_{AB} is the Adams-Bohart kinetic constant ($\text{l mg}^{-1} \text{min}^{-1}$), N_o is the saturation concentration (mg l^{-1}). From this equation, values describing the characteristic operational parameters of the column can be determined from a plot of $\ln \left(\frac{C_o}{C_t} - 1 \right)$ against t at a given bed depth and flow rate.

The Adams-Bohart plots obtained after applying Equation 5 to the experimental data are shown in Figure 9 and linear relationships were obtained for the relative concentration region up to 0.5, i.e. up to 50% breakthrough, for all breakthrough curves. The kinetic constant (K_{AB}) and saturation concentration (N_o) values were calculated from the slope and intercept of the curves, respectively, and are given in Table 2. In all cases, the values of K_{AB} decreased with increase in initial metal concentration as well as flow rate, and increased with increase in bed depth. Since the Adams-Bohart model assumes that surface reaction is the rate-limiting step, the variation of the kinetic parameter, K_{AB} , with operational conditions indicates that the sorption process for the metal ions was significantly controlled by mass transfer rather than surface reaction [27]. When mass transfer limitation is present, the rate constant K_{AB} is no longer constant, but becomes a lumped rate constant containing the effects of both the intrinsic kinetics and mass transport.

Thomas model: The linearized form of the Thomas model can be described by the following expression [28,29]:

$$\ln \left(\frac{C_o}{C_t} - 1 \right) = \frac{k_{TH} q_o m}{Q} - k_{TH} C_o t \quad (6)$$

where K_{TH} is the Thomas rate constant (ml/min mg), q_o is the adsorption capacity (mg/g) and t stands for total flow time (min). From Eq. (6), the values of K_{TH} and q_o can be determined from the linear plot of $\ln \left(\frac{C_o}{C_t} - 1 \right)$ against t . The Thomas model is suitable for adsorption process where the

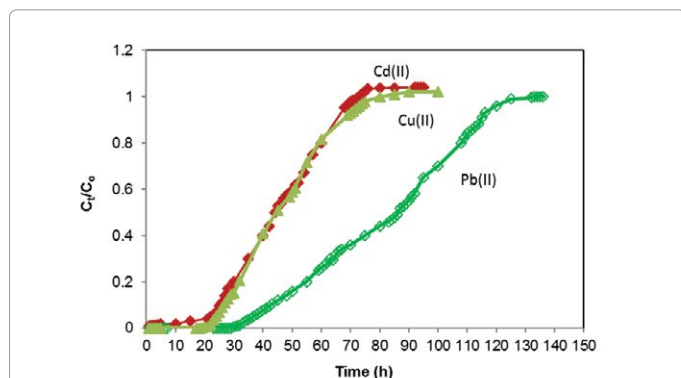


Figure 8: Breakthrough curves showing outlet Pb(II), Cu(II) and Cd(II) concentration normalised to inlet concentration vs time.

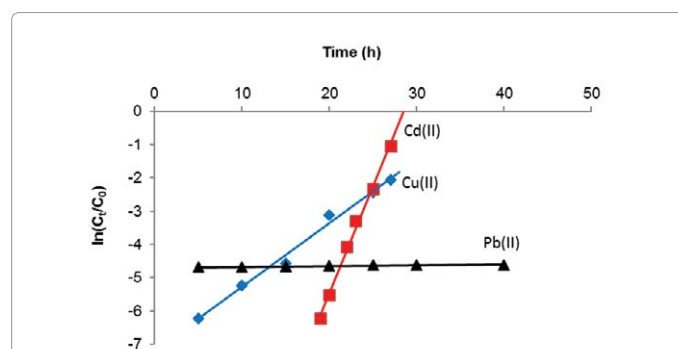


Figure 9: Adams-Bohart model plots for Cu(II), Cd(II) and Pb(II) ions (concentration of metal ions, 10 mg/L; bed depth, 2 cm; flowrate, 10 ml/min). C_o and C_t are the inlet and outlet metal ions concentrations respectively.

Parameter	(l/mg min)	(mg/l)	R ²
Pb(II) Flow rate (ml/min)			
2	29.4 × 10 ⁻⁴	6601	0.8
10	13.5 × 10 ⁻⁴	9856	0.9
20	7.4 × 10 ⁻⁴	11253	0.9
Initial Pb(II) concentration (mg/l)			
10	13.5 × 10 ⁻⁴	9856	0.9
50	12.3 × 10 ⁻⁴	10125	0.9
100	5.75 × 10 ⁻⁴	13253	0.9
Column bed depth (cm)			
1.5	6.23 × 10 ⁻⁴	10958	0.9
2	13.5 × 10 ⁻⁴	9856	0.9
2.5	14.6 × 10 ⁻⁴	7127	0.9
Cu(II) Flow rate (ml/min)			
2	7.82 × 10 ⁻²	215	0.9
10	3.91 × 10 ⁻²	875	0.9
20	1.12 × 10 ⁻²	1201	0.9
Initial Cu(II) concentration (mg/l)			
10	1.91 × 10 ⁻²	875	0.9
50	1.52 × 10 ⁻²	1256	0.9
100	8.32 × 10 ⁻³	7692	0.9
Column bed depth (cm)			
1.5	1.22 × 10 ⁻²	1231	0.9
2	1.91 × 10 ⁻²	875	0.9
2.5	8.63 × 10 ⁻²	525	0.9
Cd(II) Flow rate (ml/min)			
2	13.35 × 10 ⁻²	152	0.9
10	6.43 × 10 ⁻²	286	0.9
20	1.33 × 10 ⁻²	798	0.9
Initial Cd(II) concentration (mg/l)			
10	6.43 × 10 ⁻²	286	0.9
50	2.55 × 10 ⁻²	755	0.9
100	1.01 × 10 ⁻²	1201	0.9
Column bed depth (cm)			
1.5	2.35 × 10 ⁻²	589	0.9
2	6.43 × 10 ⁻²	286	0.9
2.5	9.89 × 10 ⁻²	107	0.9

Table 2: Adams-Bohart model parameters.

external and internal diffusion will not be the limiting step. From Figure 10, it was shown that the Thomas model (range from 0.95 to 0.99) provided a better fitting compared to Adams-Bohart model (R² range from 0.83 to 0.93). An inadequacy of the Adams-Bohart model arises when the isotherm under study exhibits Langmuir equilibrium characteristics which, under certain conditions cannot be approximated by a rectangular isotherm [28,29]. It can be seen from Table 3 that the value of q_0 increased with increasing bed depth and flow rate. However, the value of K_{TH} decreased with bed depth for all the metals studied. Furthermore, the value of K_{TH} decreased while the value of q_0 increased as the initial metal concentration increased. These observations were attributed to the driving force for adsorption in the concentration difference. The lower flow rate, higher influent concentration and higher bed depth would increase the adsorption of Pb(II), Cd(II) and Cu(II) onto the *H. ranunculoides* column. It can also be seen in Table 3 that the trend in q_0 values obtained in column sorption, (Pb(II)>Cu(II)>Cd(II)) is similar to the trend in batch sorption experiments (Table 1). It can further be seen from comparison of batch and continuous flow data that the sorption capacities obtained followed the trend: q_{max} values- Pb(II) (22.25 mg/g)>Cu(II) (12.55 mg/g)>Cd(II) (11.45

mg/g); N_0 values- Pb(II) (6601 mg/l)>>Cu(II) (215 mg/l)>Cd(II) (152

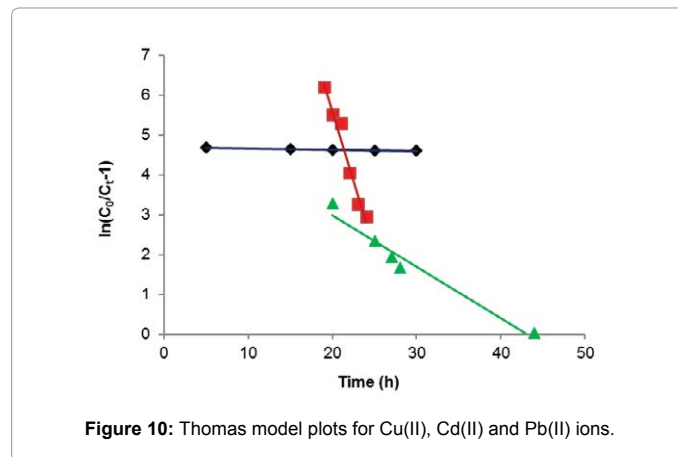


Figure 10: Thomas model plots for Cu(II), Cd(II) and Pb(II) ions.

Parameter	(×10 ⁻⁴ mL/min mg)	(mg/g)	
Pb(II)			
Flow rate (ml min ⁻¹)			
2	0.01	1,25,602.31	1
10	0.05	94,101.25	1
20	0.12	61,321.28	1
Initial Pb(II) concentration (mg l ⁻¹)			
10	0.05	94,101.25	1
50	0.01	96,771.82	1
100	0.008	98,811.36	1
Column bed depth (cm)			
1.5	2.13	70,211.73	1
2	0.05	94,101.25	1
2.5	0.01	95,526.85	1
Cu(II)			
Flow rate (ml min ⁻¹)			
2	0.51	6,489.71	1
10	2.21	2,532.56	1
20	5.32	1,235.45	1
Initial Cu(II) concentration (mg l ⁻¹)			
10	2.21	811.62	1
50	0.15	1,102.61	1
100	0.05	2,532.56	1
Column bed depth (cm)			
1.5	5.75	1,101.25	1
2	2.21	2,532.56	1
2.5	1.13	5,175.61	1
Cd(II)			
Flow rate (ml min ⁻¹)			
2	2.51	3,756.85	1
10	12.15	1,625.78	1
20	16.89	989.36	1
Initial Cd(II) concentration (mg l ⁻¹)			
10	12.15	1,625.78	1
50	5.02	2,811.75	1
100	1.01	2,989.65	1
Column bed depth (cm)			
1.5	14.12	3,110.27	1
2	12.15	1,625.78	1
2.5	9.35	899.36	1

Table 3: Thomas model parameters.

mg/l); and q_0 values- Pb(II) (61321.28~125602.31 mg/g)>>Cu(II) (1235.45~6489.71 mg/g)>Cd(II) (989.36~3756.85 mg/g) for the batch and continuous-flow systems, respectively. These results clearly indicate the higher sorption capacity for Pb(II) compared to the other two metal ions. However, q_0 values are significantly different from q_{max} and this observation was further probed by calculating values of q_0 at breakthrough ($q_{0.5}$) and saturation points (q_s). As an illustration, was calculated as follows:

$$q_{0.5} = \frac{\text{breakthrough time (at 50\%)} \times \text{flowrate} \times \text{feed concentration}}{\text{Mass of adsorbent in bed (g)}}$$

At breakthrough times of 20, 22 and 35 h for Cd(II), Cu(II) and Pb(II) respectively, flow rate of 10 ml/min, initial metal concentration of 10 mg/L and adsorbent mass of 35.5 g, $q_{0.5}$ values of 3.38, 3.72 and 5.92 mg/g were obtained for Cd(II), Cu(II) and Pb(II) respectively. Saturation adsorption capacities (q_s) of 17.26, 21.2 and 28.24 mg/g were obtained for Cd(II), Cu(II) and Pb(II) at saturation times of 75, 90 and 120 h, respectively. It is interesting to note that these values of q_s were comparable to q_{max} obtained in single metal system from Langmuir model.

Conditions: concentration of metal ions 10 mg/L, bed depth 2 cm, flowrate 10 ml/min. C_o and C_t are the inlet and outlet metal ions concentrations respectively.

Conclusions

This paper presented findings from a detailed study of the adsorption of Pb(II), Cu(II) and Cd(II) ions using an abundantly available material: *H. ranunculoides*. Experiments were carried out in batch and continuous flow systems. Results from single-metal sorption experiments showed that the adsorption trend followed the order: Pb(II)>Cu(II)>Cd(II). In binary systems, the highest inhibition capacity was for Pb(II) ions in the presence of Cd(II) ions, whereas the lowest was for Cd(II) ions in the presence of Pb(II) ions. Furthermore, it was shown that Pb(II) ions could still be effectively removed in the presence of either Cu(II) or Cd(II) ions and the competition in sorption of the heavy metals was affected by the relative concentration of the interfering metal. Continuous flow studies revealed that the Thomas model provided a better fit to the experimental data than the Adams-Bohart model and it was concluded that mass transfer, i.e. external diffusion was not the rate limiting step during the removal of Pb(II), Cu(II) and Cd(II) by immobilised *H. ranunculoides*.

Acknowledgements

The International Foundation for Science, Stockholm, Sweden supported this research, through Grant Number W/4266-2 to Courtie Mahamadi.

References

- Crini G (2005) Recent developments in polysaccharide-based materials used as adsorbents in wastewater treatment. Prog Polym Sci 1: 38-70.
- Gadd GM (2009) Heavy metal pollutants: environmental and biotechnological aspects. In: Schaechter M (ed) Encyclopedia of microbiology, Elsevier, Oxford pp 321-334
- Yu J, Tong M, Sun S, Li B (2007) Cystine-modified biomass for Cd (II) and Pb (II) biosorption. J Hazard Mat 143: 277-284.
- Vegliò F, Beolchini F (1997) Removal of metal by biosorption: a review. Hydrometallurgy 44: 301-316.
- Laus R, Tadeu de Fávère VT (2011) Competitive adsorption of Cu(II) and Cd(II) ions by chitosan crosslinked with epichlorohydrin-triphosphate. Bioresour Technol 102: 8769-8776.
- Yan C, Li G, Xue P, Wei Q, Li Q (2010) Competitive effect of Cu(II) and Zn(II) on the biosorption of lead(II) by *Myriophyllum spicatum*. J Hazard Mater 179: 721-728.
- Ma P, Zhang D, He H (2009) Effect of competitive interference on biosorption of cadmium by immobilized *Lentinus edodes* residue. Desalin Water Treat 12: 292-298.
- Helios-Rybicka E, Wójcik R (2012) Competitive sorption/desorption of Zn, Cd, Pb, Ni, Cu, and Cr by clay-bearing mining wastes. Appl Clay Sci 65-66: 6-13.
- Liang S, Guo X, Tian Q (2011) Adsorption of Pb²⁺ and Zn²⁺ from aqueous solutions by sulfured orange peel. Desalination 275: 212-216.
- Moreno-Piraján JC, Gómez-Cruza R, García-Cuello VS, Giraldo L (2010) Binary system Cu(II)/Pb(II) adsorption on activated carbon obtained by pyrolysis of cow bone study. J Anal Appl Pyrol 89: 122-128.
- Depci T, Kul AR, Önal Y (2012) Competitive adsorption of lead and zinc from aqueous solution on activated carbon prepared from Van apple pulp: Study in single-and multi-solute systems. Chem Eng J 200-202: 224-236.
- Mahamadi C, Nharingo T (2010) Competitive adsorption of Pb²⁺, Cd²⁺ and Zn²⁺ ions onto *Eichhornia crassipes* in binary and ternary systems. Bioresour Technol 101: 859-864.
- Zhu Y., Hu J, Wang J (2012) Competitive adsorption of Pb(II), Cu(II) and Zn(II) onto xanthate-modified magnetic chitosan. J Hazard Mater 221-222: 155-161.
- Sulaymon AH, Yousif, SA, Al-Faize MM (2013) Competitive Biosorption of Lead, Mercury, Chromium and Arsenic Ions onto Activated Sludge in Batch Adsorber. Aquat Sci Technol 1: 30-51.
- Vullo DL, Ceretti HM, Daniel MA, Ramirez SA, Zalts A (2008) Cadmium, zinc and copper biosorption mediated by *Pseudomonas veronii* 2E. Bioresour Technol 99: 5574-5581.
- Volesky B (2001) Detoxification of metal bearing effluents: biosorption for the next century. Hydrometallurgy 59: 203-216.
- Vijayaraghavan T, Yuan G (2001) Heavy metal removal in a biosorption column by Immobilised *M. rouxii* biomass. Bioresour Technol 78: 243-249.
- Ofomaja AE, Ho Y (2008) Effect of temperatures and pH on methyl violet biosorption by *Mansonia* wood sawdust. Bioresour Technol 99: 5411-5417.
- Liu QS, Zhen T, Wang P, Guo L (2010) Preparation and characterization of activated carbon from bamboo by microwave-induced phosphoric acid activation. Ind Crop Prod 31: 233-238.
- Igberase E, Osifo P, Ofomaja A (2014) The adsorption of copper(II) ions by polyaniline graft chitosan beads from aqueous solution: Equilibrium, kinetic and desorption studies. J Env Chem Eng 2: 362-369.
- Ofomaja AE, Unuabonah EI, Oladoja NA (2010) Competitive modeling for the biosorptive removal of copper and lead ions from aqueous solution by *Mansonia* wood sawdust. Bioresour Technol 101: 3844-3852.
- Zamil SS, Ahmad S, Choi MH, Park JY, Yoon SC (2009) Correlating metal ionic characteristics with biosorption capacity of *Staphylococcus saprophyticus* BMSZ711 using QICAR model. Bioresour Technol 100: 1895-1902.
- Ibrahim M, Kühn O, Scheytt T (2009) Molecular Spectroscopic study of water hyacinth dry matter. Open Chem Phys J 2: 1-6.
- Weber WJ, Digiano FA (1996) Process dynamics in Environmental systems: Environmental Science and Technology Service. Wiley and Sons, New York.
- Kumar PA, Chakraborty S (2009) Fixed-bed column study for hexavalent chromium removal and recovery by short-chain polyaniline synthesized on jute fiber. J Hazard Mater 162: 1086-1098.
- Ahmad AA, Hameed BH (2010) Fixed-bed adsorption of reactive azo dye onto granular activated carbon prepared from waste. J Hazard Mater 175: 298-303.
- Chu KH (2010) Fixed bed sorption: Setting the record straight on the Bohart-Adams and Thomas models. J Hazard Mater 177: 1006-1012.
- Thomas HC (1994) Heterogeneous ion exchange in a flowing system. J Am Chem Soc 66: 1664-1666.
- Chen SH, Yue QY, Gao BY, Li Q, Xu X (2011b) Removal of Cr(VI) from aqueous solution using modified corn stalks: characteristic, equilibrium, kinetic and thermodynamic study, Chem Eng J 168: 909-917.